Strong Support for the Millisecond Pulsar Origin of the Galactic Center GeV Excess

Richard Bartels,[*] Suraj Krishnamurthy,[†] and Christoph Weniger[‡]

GRAPPA Institute, University of Amsterdam, Science Park 904, 1090 GL Amsterdam, Netherlands

Using γ-ray data from the *Fermi* Large Area Telescope, various groups have identified a clear excess emission in the Inner Galaxy, at energies around a few GeV. This excess resembles remarkably well a signal from dark-matter annihilation. One of the most compelling astrophysical interpretations is that the excess is caused by the combined effect of a previously undetected population of dim γ-ray sources. Because of their spectral similarity, the best candidates are millisecond pulsars. Here, we search for this hypothetical source population, using a novel approach based on wavelet decomposition of the γ-ray sky and the statistics of Gaussian random fields. Using almost seven years of *Fermi*-LAT data, we detect a clustering of photons as predicted for the hypothetical population of millisecond pulsar, with a statistical significance of 10.0σ. For plausible values of the luminosity function, this population explains 100% of the observed excess emission. We argue that other extragalactic or Galactic sources, a mismodeling of Galactic diffuse emission, or the thick-disk population of pulsars are unlikely to account for this observation.

Introduction.—Since its launch in 2008, the *Fermi* Large Area Telescope (LAT) has revolutionized our understanding of the γ-ray sky. Among the major successes are the detection of more than 3000 γ-ray sources [1], the discovery of the *Fermi* bubbles [2], some of the most stringent limits on dark-matter annihilation [3], and, most recently, the detection of cross-correlations between the extragalactic γ-ray background and various galaxy catalogs [4].

One of the most interesting γ-ray signatures identified in the *Fermi*-LAT data by various groups [5–16], is an excess emission in the Inner Galaxy at energies around a few GeV. This excess attracted great attention because it has properties typical for a dark-matter annihilation signal. This Galactic Center excess (GCE) is detected both within the inner 10 arcmin of the Galactic Center (GC) [7,9,10] and up to Galactic latitudes of more than $10°$ [13,15,17,18]. It features a remarkably uniform spectrum and approximately spherical symmetry [13,15]. Proposed diffuse emission mechanisms, like leptonic or hadronic outbursts [19–21] or cosmic-ray injection in the central molecular zone [22], potentially explain part of the excess emission. However, it is challenging to explain *all* of the above aspects of the GCE with these mechanisms alone.

Probably the most plausible astrophysical interpretation for the GCE is the combined emission from a large number of unresolved millisecond pulsars (MSPs) in the Galactic bulge region [10,12,23,24]. MSPs feature a spectrum compatible with the GCE emission [15], and a large unresolved component can naturally explain the uniformity of the GCE spectrum in different regions of the sky. Recently, it was shown that the spatial distribution of MSPs that were spilled out of disrupted globular clusters can explain the morphology of the GCE [25]. Such MSPs from disrupted globular clusters have also been suggested

as the source behind the GeV through TeV emission in the inner few parsec of the GC [26]. Further possible support for the MSP hypothesis might come from *Chandra* observations of low-mass x-ray binaries (which are progenitor systems of MSPs) in M31, which show a centrally peaked profile in the inner 2 kpc [27,28], as well as the recent observation of extended hard-x-ray emission from the Galactic Center by *NuSTAR* [29].

It was claimed that an interpretation of 100% of the GCE emission in terms of MSPs would be already ruled out: a sizeable fraction of the required 10^3–10^4 MSPs should have been already detected by the *Fermi* LAT [30,31], but no (isolated) MSP has been identified so far in the bulge region. This conclusion depends crucially, however, on the adopted γ-ray luminosity of the brightest MSPs in the bulge population, on the effective source sensitivity of *Fermi* LAT, and on the treatment of unassociated sources in the Inner Galaxy [25,32]. A realistic sensitivity study for MSPs in the context of the GeV excess, taking into account all these effects, was lacking in the literature up to now (but see Ref. [33]).

In this Letter, we close this gap and present a novel technique for the analysis of dim γ-ray sources and apply it to *Fermi*-LAT observations of the Inner Galaxy. Our method is based on the statistics of maxima in the wavelet-transformed γ-ray sky (in the context of *Fermi*-LAT data, wavelet transforms were used previously for the identification of point source seeds [1,16]). We search for contributions from a large number of dim MSP-like sources, assuming that they are spatially distributed as suggested by GCE observations. Our method has several advantages with respect to previously proposed techniques based on one-point fluctuations [34], most notably, the independence from Galactic diffuse emission models and the ability for candidate source localization.

Modeling.—We simulate a population of MSP-like sources, which we hereafter refer to simply as the *central source population* (CSP), distributed around the GC at 8.5 kpc distance from the Sun. The CSP is taken to have a spatial distribution that follows a radial power law with an index of $\Gamma = -2.5$ and a hard cutoff at radius $r = 3$ kpc [13,15]. As a reference γ-ray energy spectrum, we adopt the stacked MSP spectrum from Ref. [35], $(dN/dE) \propto e^{-E/3.78\,\text{GeV}}E^{-1.57}$. The γ-ray luminosity function is modeled with a power law, $(dN/dL) \propto L^{-\alpha}$, with index $\alpha = -1.5$ [32,35–37], and with lower and upper hard cutoffs at $L_{\min} = 10^{29}$ erg s^{-1} and $L_{\max} = 10^{34}$–10^{36} erg s^{-1}, respectively. Luminosities are integrated over 0.1–100 GeV. Our results depend little on $L_{\min}$. Given that only about 70 MSPs have been detected in γ rays up to now [33], $L_{\max}$ is not well constrained. The γ-ray luminosity of the brightest observed MSP is somewhere in the range $(0.5–2) \times 10^{35}$ erg s^{-1} [33,35], depending on the adopted source distance [25,32]. Diffuse emission is modeled with the standard model for point source analysis `gll_iem_v06.fits` and the corresponding isotropic background.

Data.—For our analysis, we use almost seven years of ultraclean *Fermi*-LAT P8R2 data taken between August 4, 2008 and June 3, 2015 (we find similar results for source class data). We select both front- and back-converted events in the energy range 1–4 GeV, which covers the peak of the GCE spectrum. The region of interest (ROI) covers the Inner Galaxy and spans Galactic longitudes $|\ell| \leq 12°$ and latitudes $2° \leq |b| \leq 12°$. The data are binned in Cartesian coordinates with a pixel size of 0.1°.

Wavelet peaks.—The wavelet transform of the γ-ray data is defined as the convolution of the photon count map, $\mathcal{C}(\Omega)$, with the wavelet kernel, $\mathcal{W}(\Omega)$,

$$\mathcal{F}_{\mathcal{W}}[\mathcal{C}](\Omega) \equiv \int d\Omega' \mathcal{W}(\Omega - \Omega')\mathcal{C}(\Omega'), \quad (1)$$

where Ω denotes Galactic coordinates [38] [note that $\int d\Omega \mathcal{W}(\Omega) = 0$]. The central observable for the current analysis is the *signal-to-noise ratio* (SNR) of the wavelet transform, which we define as

$$\mathcal{S}(\Omega) \equiv \frac{\mathcal{F}_{\mathcal{W}}[\mathcal{C}](\Omega)}{\sqrt{\mathcal{F}_{\mathcal{W}^2}[\mathcal{C}](\Omega)}}, \quad (2)$$

where in the denominator the wavelet kernel is squared before performing the convolution. If the γ-ray flux varied only on scales much larger than the extent of the wavelet kernel, and in the limit of a large number of photons, $\mathcal{S}(\Omega)$ would behave like a smoothed Gaussian random field. Consequentially, $\mathcal{S}(\Omega)$ can be loosely interpreted as the local significance for having a source at position Ω in units of standard deviations.

As the wavelet kernel, we adopt the second member of the Mexican hat wavelet family, which was shown to provide very good source discrimination power [39] and which was used for the identification of compact sources in Planck data [40]. The wavelet can be obtained by a successive application of the Laplacian operator to a two-dimensional Gaussian distribution with width $\sigma_b R$. Here, $\sigma_b = 0.4°$ corresponds to the *Fermi*-LAT angular resolution at 1–4 GeV, and R is a tuning parameter. We find best results when R varies linearly with latitude from $R = 0.53$ at $b = 0°$ to $R = 0.83$ at $b = \pm 12°$. This compensates to some degree the increasing diffuse backgrounds towards the Galactic disk, while optimizing the source sensitivity at higher latitudes [40].

The resulting SNR of the wavelet transform $\mathcal{S}(\Omega)$ is shown in Fig. 1. As expected, the Galactic diffuse emission is almost completely filtered out by the wavelet transform, whereas bright sources lead to pronounced peaks. We adopt a simple algorithm for peak identification: we find all pixels in $\mathcal{S}(\Omega)$ with values larger than in the four adjacent pixels. We then clean these results from artifacts by forming clusters of peaks with cophenetic distances less than 0.3° and only keep the most significant peak in each cluster.

In Fig. 1, we show the identified wavelet peaks with peak significance $\mathcal{S} > 2$, as well as all 3FGL sources for comparison [1]. For sources that are bright enough in the adopted energy range, we find a good correspondence
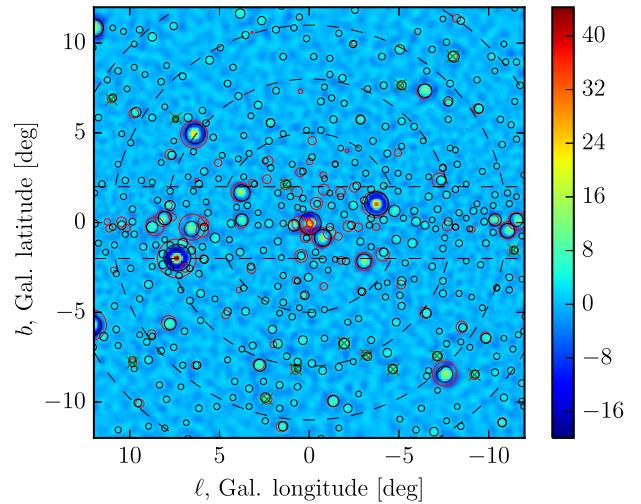

FIG. 1. SNR of the wavelet transform of γ rays with energies in the range 1–4 GeV, $\mathcal{S}(\Omega)$. The black circles show the position of wavelet peaks with $\mathcal{S} \geq 2$; the red circles show the position of third Fermi-LAT catalog (3FGL) sources. In both cases, the circle area scales with the significance of the source detection in that energy range. The dashed lines indicate the regions that we use for the binned likelihood analysis, where latitudes $|b| < 2°$ are excluded because of the strong emission from the Galactic disk. The subset of 3FGL sources that remains unmasked in our analysis is indicated by the green crosses.

between wavelet peaks and the 3FGL, both in terms of position and significance (we compare the significance of wavelet peaks $\mathcal{S}$ with the 1–3 GeV detection significance for 3FGL sources).

It is worth emphasizing that for the adopted spherically symmetric and centrally peaked distribution of the CSP, most of the sources would be detected not directly at the GC but a few degrees away from the Galactic disk. This is simply due to the much weaker diffuse emission at higher latitudes. Our focus on latitudes $|b| \geq 2°$, thus, avoids regions where source detection becomes less efficient due to strong diffuse foregrounds, without significant sensitivity loss for the source population of interest.

3FGL sources.—Before studying the statistics of the wavelet peaks in detail below, we remove almost all peaks that correspond to the known 3FGL sources based on a 0.3° (1° for $\sqrt{TS} \geq 50$) proximity cut. However, in order to mitigate a potential bias on L_{max}, we do not mask peaks that correspond to 3FGL sources that are likely part of the CSP. We identify such *MSP candidate sources* by requiring that they (i) are tagged as unassociated, (ii) show no indication for variability, and (iii) have a spectrum compatible with MSPs. The last criterion is tested by performing a χ^2 fit of the above MSP reference spectrum to the spectrum given in the 3FGL (0.1–100 GeV; five energy bins). Only the normalization is left free to vary. We require a fit quality of $\chi^2/\text{DOF} \leq 1.22$ (with DOF $= 4$) corresponding to a p value ≥ 0.3.

We find 13 3FGL sources in the Inner Galaxy ROI that pass the above MSP cuts (listed in the Supplemental Material [41]). Interestingly, the average number of MSP candidate sources in same-sized control regions along the Galactic disk in the range $|\ell| = 12°–60°$ is significantly smaller, with an average of 3.1. It is tempting to interpret this excess of MSP candidate sources in the Inner Galaxy as being caused by the brightest sources of the CSP, above the less-pronounced thick-disk population of MSPs [42,43]. However, we emphasize that the status of these 13 sources is currently neither clear nor qualitatively decisive for our results. Whether we mask them plays a minor role in the detection of the CSP below (but it does affect the inferred values for L_{max}; see the Supplemental Material [41]).

Statistical analysis.—In Fig. 2 we show a histogram of the wavelet peaks in our ROI. We bin the peaks in a two-dimensional grid, which spans the projected angle from the Galactic Center 2°–17° and wavelet peak significances in the range 1–10. The bin edges are as indicated in the figure. As expected, photon shot noise gives rise to a large number of peaks with low significances $\mathcal{S} \leq 3$, and only a small number of peaks has $\mathcal{S} \geq 5$.

We assume that the number of peaks in each bin in Fig. 2 follows—in repeated experiments and random realizations of the CSP—to a good approximation a Poisson distribution. We estimate the corresponding average number of expected wavelet peaks in each bin using a large number of Monte Carlo simulations, where we simulate the diffuse
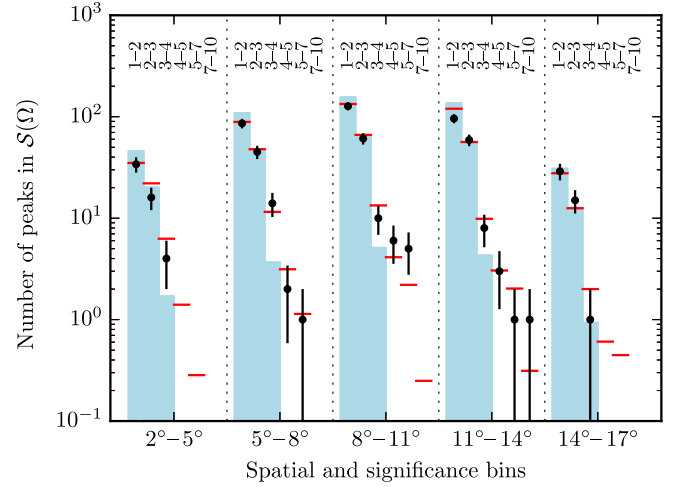

FIG. 2. Histogram of observed peaks in $\mathcal{S}(\Omega)$ in bins of projected radial distance from the GC and SNR values (black dots with statistical error bars). We show the expectation value for the case of a negligible CSP as blue bars, whereas the expectation values for the best fit are shown in red.

background emission, random realizations of the source population, and photon shot noise.

In order to quantify what CSP luminosity function reproduces best the observations, we perform a binned Poisson likelihood analysis of the wavelet peak distribution. The likelihood function is given by

$$\mathcal{L} = \prod_{i=1}^{n_r} \prod_{j=1}^{n_s} \mathcal{P}(c_{ij} | \mu_{ij}(L_{max}, \Phi_5)), \tag{3}$$

where n_r and n_s are, respectively, the numbers of radial and peak SNR bins, c_{ij} is the observed and μ_{ij} the expected number of peaks, and $\mathcal{P}$ is a Poisson distribution. The expectation values depend directly on the maximal luminosity, L_{max}, as well as on the number of simulated sources, n. To ease comparison with the literature, we determine n as a function of Φ_5, which denotes the mean differential intensity of the CSP at $b = \pm 5°$, $\ell = 0°$, and 2 GeV. In the case of the GCE, this value was found to be $\Phi_5^{\text{GCE}} = (8.5 \pm 1.5) \times 10^{-7}$ GeV^{-1} cm^{-2} s^{-1} sr^{-1} at 95.4% C.L. [15].

Results.—In Fig. 2, we show the expectation values that we obtain when neglecting contributions from the CSP (and any other nondiffuse emission). This corresponds to good approximation to the case where the GCE is of truly diffuse origin, including the case of DM annihilation or outburst events. We find that the observed number of wavelet peaks with $\mathcal{S} < 2$ is significantly lower than expected, whereas the observed number of peaks with $\mathcal{S} > 3$ is significantly higher. As we will show next, this is precisely the effect that is caused by a dim source population.

We now turn to the case with a nonzero CSP contribution. In Fig. 3, we show the limits that we obtain on the two
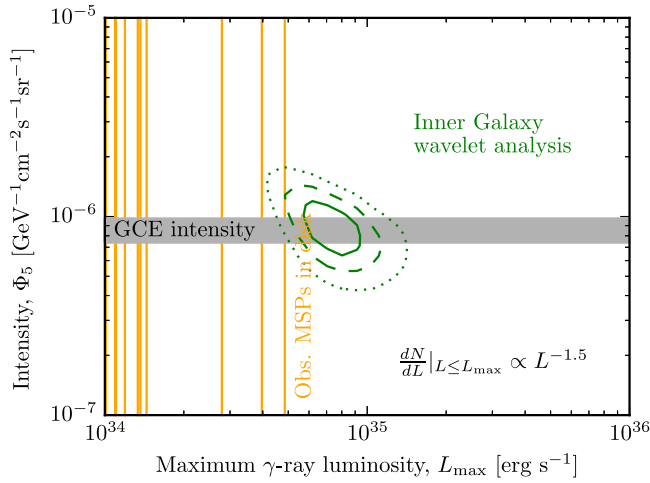
FIG. 3.   Constraints on the maximum γ-ray luminosity of the CSP, L_{max}, and the population averaged intensity at $b = \pm5°$, $\ell = 0°$, and 2 GeV, Φ_5, as derived from our wavelet analysis. We show 68.7%, 95.4%, and 99.7% C.L. contours. We also indicate the values of Φ_5 where the source population can explain 100% of the GCE (horizontal gray band, 95.4% C.L.) and as vertical orange lines the luminosity of the brightest observed nearby MSPs.

CSP parameters when fitting the histogram in Fig. 2 as described above. We find that a nonzero contribution from the CSP is favored at the level of at least 10.0σ. (When quoting the statistical significance, we conservatively take into account bins with $\mathcal{S} < 5$ only, which are most affected by a dim source population and least affected by the masking of 3FGL sources [see the Supplemental Material [41] for details]). The best-fit value for the total differential intensity is $\Phi_5 = (9.0 \pm 1.9) \times 10^{-7}\,\mathrm{GeV^{-1}\,cm^{-2}\,s^{-1}\,sr^{-1}}$ and for the maximum luminosity $L_{max} = (7.0 \pm 1.0) \times 10^{34}\,\mathrm{erg\,s^{-1}}$. As can be seen in Fig. 2, we obtain in this case a very good fit to the data.

Our preferred range of the maximum γ-ray luminosities reaches up to $L_{max} \leq 1.04 \times 10^{35}\,\mathrm{erg\,s^{-1}}$ (at 95.4% C.L.), which is compatible with observations of nearby MSPs. We illustrate this by showing in Fig. 3 the γ-ray luminosity of the brightest individually observed nearby MSPs as given in Ref. [35]. (We only show objects where second γ-ray pulsar catalog [33] distances are available; see Ref. [25] for a detailed discussion about distance uncertainties.) Furthermore, for the adopted slope of the luminosity function $\alpha = 1.5$, the best-fit value for the total differential intensity of the CSP Φ_5 is consistent with the CSP accounting for 100% of the GCE emission.

Discussion and conclusions.—We found corroborating evidence for the hypothesis that the GCE is caused by a hitherto undetected population of MSP-like sources. We performed a wavelet transform of the γ-ray emission from the Inner Galaxy, which removes Galactic diffuse emission and enhances point sources, and we studied the statistics of the peaks in this transform. We detected with 10.0σ

significance a suppression (enhancement) of low- (high-) significance wavelet peaks, relative to the expectations for purely diffuse emission. We showed that this effect is caused by the presence of a large number of dim point sources. The spatial distribution of wavelet peaks in the Inner Galaxy is compatible with a centrally peaked source distribution, and the inferred cutoff of the γ-ray luminosity function of these sources agrees with the observation of nearby MSPs. This source population can, for reasonable slopes of the luminosity function, account for 100% of the GCE emission.

For the purpose of this Letter, which introduces a novel technique, we kept our analysis as simple as possible. In general, one might worry that our results could be affected by the presence of extragalactic and Galactic sources, by the thick-disk population of MSPs and young pulsars, by the details of masking and unmasking 3FGL sources, by the details of the adopted γ-ray luminosity function, and by unmodeled substructure in the Galactic diffuse emission that is not removed by the wavelet transform. We address all of these points in the Supplemental Material [41] and show that it is rather unlikely that they affect our results qualitatively, although quantitative changes in the obtained best-fit values for Φ_5 and L_{max} are possible. In particular, we showed that the wavelet signal expected from the thick-disk population of MSPs is an order of magnitude weaker than what we actually observed and that interpretations related to unmodeled gas remain, on closer inspection, unlikely.

The prospects for fully establishing the MSP interpretation within the coming decade are very good. Our results suggested that upcoming γ-ray observations with improved angular resolution (planned or proposed γ-ray satellites like GAMMA-400 [44], ASTROGAM, and PANGU [45]) will allow us to detect many more of the bulge sources and study their distribution and spectra. For current radio instruments, it remains rather challenging to detect a MSP population in the bulge [25], but prospects for next-generation instruments are good.

Note added in proof.—Recently, we became aware of another group studying dim γ-ray sources in the Inner Galaxy, using non-Poissonian photon statistics [46].

*r.t.bartels@uva.nl
†s.krishnamurthy@uva.nl
‡c.weniger@uva.nl

[1] F. Acero *et al.* Fermi-LAT Collaboration, arXiv:1501.02003 [Astrophys. J. Suppl. Ser. (to be published)].

[2] M. Su, T. R. Slatyer, and D. P. Finkbeiner, Astrophys. J. **724**, 1044 (2010).

[3] M. Ackermann *et al.* (Fermi-LAT Collaboration), Astrophys. J. **809**, L4 (2015).

[4] J.-Q. Xia, A. Cuoco, E. Branchini, and M. Viel, Astrophys. J. Suppl. Ser. **217**, 15 (2015).

[5] L. Goodenough and D. Hooper, arXiv:0910.2998.

[6] V. Vitale and A. Morselli (Fermi-LAT Collaboration), arXiv:0912.3828.

[7] D. Hooper and L. Goodenough, Phys. Lett. B **697**, 412 (2011).

[8] D. Hooper and T. Linden, Phys. Rev. D **84**, 123005 (2011).

[9] K. N. Abazajian and M. Kaplinghat, Phys. Rev. D **86**, 083511 (2012).

[10] C. Gordon and O. Macias, Phys. Rev. D **88**, 083521 (2013).

[11] O. Macias and C. Gordon, Phys. Rev. D **89**, 063515 (2014).

[12] K. N. Abazajian, N. Canac, S. Horiuchi, and M. Kaplinghat, Phys. Rev. D **90**, 023526 (2014).

[13] T. Daylan, D. P. Finkbeiner, D. Hooper, T. Linden, S. K. N. Portillo *et al.*, arXiv:1402.6703.

[14] B. Zhou, Y.-F. Liang, X. Huang, X. Li, Y.-Z. Fan, L. Feng, and J. Chang, Phys. Rev. D **91**, 123010 (2015).

[15] F. Calore, I. Cholis, and C. Weniger, J. Cosmol. Astropart. Phys. 03 (2015) 038.

[16] M. Ajello *et al.* (Fermi-LAT Collaboration), arXiv:1511.02938.

[17] D. Hooper and T. R. Slatyer, Phys. Dark Univ. **2**, 118 (2013).

[18] W.-C. Huang, A. Urbano, and W. Xue, arXiv:1307.6862.

[19] E. Carlson and S. Profumo, Phys. Rev. D **90**, 023015 (2014).

[20] J. Petrovic, P. D. Serpico, and G. Zaharijas, J. Cosmol. Astropart. Phys. 10 (2014) 052.

[21] I. Cholis, C. Evoli, F. Calore, T. Linden, C. Weniger, and D. Hooper, J. Cosmol. Astropart. Phys. 12 (2015) 005.

[22] D. Gaggero, M. Taoso, A. Urbano, M. Valli, and P. Ullio, arXiv:1507.06129.

[23] K. N. Abazajian, J. Cosmol. Astropart. Phys. 03 (2011) 010.

[24] Q. Yuan and B. Zhang, J. High Energy Astrophys. **3–4**, 1 (2014).

[25] T. D. Brandt and B. Kocsis, Astrophys. J. **812**, 15 (2015).

[26] W. Bednarek and T. Sobczak, Mon. Not. R. Astron. Soc. **435**, L14 (2013).

[27] R. Voss and M. Gilfanov, Astron. Astrophys. **468**, 49 (2007).

[28] K. N. Abazajian and M. Kaplinghat, Phys. Rev. D **86**, 083511 (2012).

[29] K. Perez *et al.*, Nature (London) **520**, 646 (2015).

[30] D. Hooper, I. Cholis, T. Linden, J. M. Siegal-Gaskins, and T. R. Slatyer, Phys. Rev. D **88**, 083009 (2013).

[31] I. Cholis, D. Hooper, and T. Linden, J. Cosmol. Astropart. Phys. 06 (2015) 043.

[32] J. Petrovi, P. D. Serpico, and G. Zaharijas, J. Cosmol. Astropart. Phys. 02 (2015) 023.

[33] A. Abdo *et al.* (Fermi-LAT Collaboration), Astrophys. J. Suppl. Ser. **208**, 17 (2013).

[34] S. K. Lee, M. Lisanti, and B. R. Safdi, J. Cosmol. Astropart. Phys. 05 (2015) 056.

[35] I. Cholis, D. Hooper, and T. Linden, arXiv:1407.5583.

[36] A. W. Strong, Astrophys. Space Sci. **309**, 35 (2007).

[37] C. Venter, T. Johnson, A. Harding, and J. Grove, arXiv:1411.0559.

[38] F. Damiani, A. Maggio, G. Micela, and S. Sciortino, Astrophys. J. **483**, 350 (1997).

[39] J. Gonzalez-Nuevo, F. Argueso, M. Lopez-Caniego, L. Toffolatti, J. Sanz, P. Vielva, and D. Herranz, Mon. Not. R. Astron. Soc. **369**, 1603 (2006).

[40] P. Ade *et al.* (Planck Collaboration), Astron. Astrophys. **571**, A28 (2014).

[41] See Supplemental Material at http://link.aps.org/supplemental/10.1103/PhysRevLett.116.051102 for discussion of the possible impact of various systematics on our results. This includes a control region analysis, a discussion of various types of γ-ray sources, substructure in diffuse emission, a thick-disk population of MSPs, sphericity and the role of negative wavelet peaks.

[42] T. Gregoire and J. Knödlseder, Astron. Astrophys. **554**, A62 (2013).

[43] F. Calore, M. Di Mauro, F. Donato, and F. Donato, Astrophys. J. **796**, 14 (2014).

[44] N. Topchiev, A. Galper, V. Bonvicini, O. Adriani, R. Aptekar *et al.*, Bull. Russ. Acad. Sci. Phys. **79**, 417 (2015).

[45] X. Wu, M. Su, A. Bravar, J. Chang, Y. Fan *et al.*, Proc. SPIE Int. Soc. Opt. Eng. **9144**, 91440F (2014).

[46] S. K. Lee, M. Lisanti, B. R. Safdi, T. R. Slatyer, and W. Xue, following Letter, Phys. Rev. Lett. **116**, 051103 (2016).